Article

A Comparison of Thermal Insulation with Interstitial Condensation in Different Climate Contexts in Existing Buildings in Europe †

Lamberto Tronchin *, Kristian Fabbri and Maria Cristina Tommasino

Architecture—DA, University of Bologna, 47521 Cesena, Italy
* Correspondence: lamberto.tronchin@unibo.it
† This paper is an extended version of the paper published in 2020 IEEE Proceedings—2020 IEEE International Conference on Environment and Electrical Engineering and 2020 IEEE Industrial and Commercial Power Systems Europe, EEEIC/I and CPS Europe 2020 Conference, Madrid, Spain, 9–12 June 2020; Article number 9160583.

Abstract: The work presented here investigates the risk of interstitial condensation between the existing masonry and the insulation using several materials and evaluates the water content inside the insulation (WCI) through various simulations in dynamic mode onto existing buildings located in different countries in Europe. The insulation materials considered are specifically: natural fibre materials, mineral fibre materials, and artificial materials. The scenarios were chosen considering different climate zones, according to the Köppen climate classification, and the analysed buildings were taken from the TABULA database in the years of construction from 1945 to 1969. The building typologies are single-family houses, where in each building system the insulation was placed towards the warm side with a fixed thickness of 5 cm. The simulations concerned: (a) the application scenario, (b) the type of stratigraphy chosen, and (c) the exposure of the existing building system. The outputs generated by the simulations provided the data to determine in which type of building, depending on the insulating materials, interstitial condensation is formed or not. It is shown that only for the climate zones of the cities of Oslo and Brussels, associated with their building typologies, for the insulating materials: mineral and natural, is there the formation of interstitial condensation

Keywords: thermo-hygrometric evaluation; interstitial condensation; thermal insulation; WUFI; TABULA; Köppen classifications

1. Introduction

The installation of insulating materials in existing buildings improves the energy performance of buildings. The scientific literature and several case studies report examples of how the increasing energy efficiency through such interventions leads to a reduction in energy needs for both heating and cooling [1–4].

Conversely, there is a lack of studies which deal with the contemporary analysis of thermal conductivity (transmittance) and thermo-hygrometric analysis within the layers. Ignoring this effect could cause heavy damage to the proposed solutions, provoking a total lack of the enhancement obtained with them. This paper aims to contribute to covering this gap in the research.

The insulating layer can be positioned on the external, intermediate, or internal side of the masonry, where the latter case is the subject of study in this article and previous research [5–7].

Moreover, in the scientific literature, some papers consider the dynamic simulation of the buildings following the EN 15026 standard, but they consider only single cases, whilst this paper covers different case studies.

Besides, this paper focuses on the validation of different scenarios applied to different building typologies described in the TABULA database and applied in different climate contexts in Europe.

In general, the research on building energy performance focuses on the reduction of energy needs, on the environmental effects caused by non-renewable energy, and on other similar themes. Following this approach, this paper focuses on the damages and the effects caused by superficial and interstitial condensation in these building structures. These effects could modify (and worsen) both the indoor quality (for example, creating moulds, micro-biological effects) and the thermophysical characteristics of the insulating layers themselves. In fact, due to the condensation, the thermal conductivity (i.e., thermal transmittance) is getting worse.

The building sector could utilise various typologies of insulating materials. These elements differ in their technical characteristics and their nature. Natural or organic materials could be utilised as a valid alternative to synthetic ones. Several studies recently carried out in this direction demonstrate that the use of materials of an organic nature, such as hemp fibre or linen fibre panels, in certain situations can effectively reduce the risk of condensation [8,9]. In particular, their use could improve the collection, production, manufacturing, and maintenance procedures. Since the latter materials are putrescible, these precautions, for the types of natural/organic materials, are important to avoid the risk of negative effects caused by humidity and free water [10]. These phenomena very often cause the greatest damage to buildings. In fact, it has been shown that humidity can be a risk to building structures and is the first cause of damage in construction (48.3%) [11].

The building typologies concerning the European real estate park enjoy similar characteristics in the historical and economic technological field [12], and therefore also from the perspective of the construction of the building elements. To help identify the type of building, it is necessary to consult the TABULA database [13] (Typology Approach for Building Stock Energy Assessment), which introduced a common methodology to define building types and to create references to building types within Europe [14].

This method allows to quantify the possible energy savings obtained by renovations. It has been demonstrated that more than 40% in terms of energy savings could be achieved through basic renovations [14]. Interventions aimed at ensuring the greatest result in terms of energy efficiency on the building envelope see the possibility to intervene in various aspects of the building. The most interesting results are associated with the renovation measures of the building envelope, such as the thermal insulation of the opaque elements of the building, where, if combined with a replacement of the windows and the heat generator, an energy saving of 65% can be achieved [1].

Nevertheless, there is a lack of research on the link among thermo-hygrometric aspects, thermal conductivity, and climate context, all considered at the same time. The scientific literature includes works on the thermal conductivity of the material or the transmittance, which could vary considering different materials or stratigraphies. Conversely, this paper focuses on the vapour resistance coefficient of different materials, including the canopy fibre materials. Our results confirm some already known results, i.e., the relation existing between natural fibre materials and a cold climate context. One of the most important outcomes of this research consists of the discovery that the materials having good conductivity values are less sensitive to the risk of a high level of relative humidity and therefore interstitial condensation.

It should be noted that not all building envelopes are suitable for energy requalification; in this regard, Ferreira et al. [15] provided a review of decision support tools for the renovation of buildings. In their paper, the authors classified the tools according to their different purposes, obtaining five groups: (1) improvement of energy and environmental performance, (2) economic analysis, (3) lifecycle assessment, (4) environmental sustainability assessment, and (5) general methods.

With reference to the improvement of energy performance, the first step consists of determining the reference building typology. For this purpose, TABULA reports a number of typologies which are linked with the period of construction. For each reference period, different construction systems are associated, each of them characterised with typical stratigraphies representing the peculiarities of the place of belonging and sorted by

different types of building elements [13,16]. A fundamental role is represented by the year of construction of the individual building types. The year of construction influences the structure of the stratigraphy which may be chosen for an energy enhancement, because the building packages have changed during the years from the technological point of view of both materials and energy. Moreover, several combined factors must be considered when choosing the reference period to be associated with an energy refurbishment intervention [15]. It has been proven [1] that the least effective redevelopment interventions in Europe, considering both the energy and economic aspects, are those applied to the most recent types of buildings, with construction periods of 1976–2005. Another important factor for an increase in the energy efficiency of the envelope is to identify the types of buildings for which such interventions can be more efficient. Additionally in this direction, it has been demonstrated that only some buildings are more functional than others. The thermal insulation of the opaque envelope in single-family houses is more effective from the energy point of view than other buildings in Europe [1,12].

The renovation work on the buildings, in any case, provides for the study of the climate in which the shell is inserted. In this regard, in Europe, the latter is predominantly continental, and there are significant variations between the south and north and between the mountainous and flat areas. For this purpose, the subdivision of climate zones according to the classification of Köppen climates (where each climate is defined for predetermined values of temperature and precipitation) [17] is useful to determine the climate zones to which to refer.

The regulatory framework at the international level proposes, in addition to the traditional method of the Glaser diagram [18] based on stationary analysis, the possibility to use dynamic hygrometric simulations. In this regard, considering the standard UNI EN 15026 [19], the analysis provided for the assessment of crevice condensation was obtained through a variable steam migration calculation using WUFI PRO software [20]. The choice to carry out the simulations through a software able to elaborate a calculation during a dynamic regime has allowed to evaluate climatic conditions closer to reality, also considering all the processes of moisture transport in materials that the stationary method is not able to consider [21]. Hygrometric simulations allow, if used correctly, to evaluate almost all phenomena relevant to building practice, such as: water absorption, precipitation, solar radiation, steam diffusion, moisture accumulation, capillary liquid transport, and many more. The difference in using a calculation software in a variable regime compared to the traditional Glaser method, moreover, involves a greater responsibility for the designer, but allows a much more complete and specific evaluation of the hygrometric behaviour of the building components [20]. For a qualitative numerical control of the results in hygrothermal terms, it is appropriate to impose a sufficiently long simulation period to allow the materials to reach hygrothermal equilibrium with the environment [6,7,20].

The objective of this article is to compare different types of insulation materials, introduced in existing building types in Europe, derived from TABULA, to obtain information about the risk of interstitial condensation and the amount of water in the insulation.

The information obtained will concern the presence or absence of crevice condensation and MWCI (kg/m^2), depending on the guidelines, and additionally, the exact timeframe (dd/mm/yyyy) at which these phenomena may develop over the 10 years of simulations. It is thus possible to determine the type of insulation, installed in a given type of building, which favours interstitial condensation and high WCI, depending on the orientation and climate zone.

2. Materials and Methods

The methodology adopted for the research involves:

1. Definition of the building typologies studied by TABULA.
2. Definition of the cities in the climatic zones of Köppen.
3. Choice of insulation materials.
4. Selection of software and orientation.
5. Application scenarios.

2.1. Definition of Building Types

For the determination of the different types of buildings, reference has been made to the TABULA WebTool [16], which provides for the introduction of some data concerning the type of building and the year of its construction. Only through the identification of these parameters is it possible to recognise the type of construction to develop the simulations in a variable regime. Once the type of construction system to be analysed was identified, the insulation in the internal part of the wall profile was introduced, with a thickness of 5 cm.

For the choice of the type of building to refer to, a search was carried out from EUROSTAT data [22], from which it emerged that, in Europe, 33.6% of the population live in independent single-family houses. Furthermore, as demonstrated [1,12], single-family houses, in the European context, lend themselves to be more effective in energy requalification interventions, which involve the insulation of the opaque shell, compared to the other building types proposed by TABULA. For these considerations, this typology has been chosen for the development of the simulations. TABULA WebTool associates the reference time period in which they have been realised to the single-building typologies. To be able to determine this, it is necessary to refer to a specific time period.

The reference period, associated with the chosen typology, has also been obtained from a search from EUROSTAT data [23] related to the period of single-family house construction in Europe. Through the research database, it was found that 26.85% of the European building stock was built between 1945 and 1969. Furthermore, during the period between 1976 and 2005, the interventions on the existing buildings were the less performing from an energy (and economic) point [1]. Comparing the two periods, it was observed that the time interval between 1945 and 1969 was preferred, both from the optimisation of the energy requalification intervention and from the percentage quantity of building typology built in that period. For these reasons, it was decided to adopt the period between 1945 and 1969 as a reference.

2.2. Cities and Climate Zones

The choice of geographical areas in which to identify the types of buildings was associated with variable data, in fact, for each location, of the six choices, there will be a different type of building resulting from TABULA. This element allows to specifically identify the wall stratigraphy to be used, as TABULA WebTool needs three fundamental data points to be able to identify the building system. Two of the data points are associated with fixed input data, in the current method, such as the year of construction and the type of building, while the third specifically concerns the geographical position in Europe, divided by member states. The choice of the reference city was determined through the geographical division of Europe into areas of northern, central, and southern. The cities specifically chosen were:

(a) Milan and Malaga for the southern Europe area.
(b) Vienna and Brussels for the central Europe area.
(c) Oslo and Hamburg for northern Europe.

Each of these cities has been assigned a climate classification of Köppen [17,24] to further subdivide them by climate zone.

2.3. Insulating Materials

This article compares different types of insulating materials, which can be distinguished from each other by their nature of origin. The materials chosen for the simulations generated are of mineral, natural/organic, and synthetic nature. The choice in using these types of insulators was due to the fact that each single material has a different behaviour in hygrothermal terms in response to the surface where it is installed [25].

The chosen insulators were:

(a) Hemp fibre and flax fibre panels (natural fibre materials).
(b) Rock wool and glass wool (mineral materials).
(c) EPS and XPS (synthetic materials).

Each single insulator differs in several aspects from each other, such as porosity (m^3/m^3), density (kg/m^3), conductivity (W/mK), and vapour permeability coefficient ($-$) (Table 1).

Table 1. Input data concerning the city of Milan, with a total of 18 numerical simulations for each location, for a total of 108 simulations in the variable regime considering all the chosen areas.

		Scenarios				Insulation Data				
City	Climate Classification According to the Köppen System	Type of Insulation	Orientation	Simulation Departure Date [dd/mm/yyyyyy]	End Date of Simulation [dd/mm/yyyyyy]	μ	ρ	λ	ε	s
MI	Cfa	Hemp fibre	North	01/10/19	01/10/29	1.5	50	0.038	0.95	5
MI	Cfa	Hemp fibre	South	01/10/19	01/10/29	1.5	50	0.038	0.95	5
MI	Cfa	Hemp fibre	East/West	01/10/19	01/10/29	1.5	50	0.038	0.95	5
MI	Cfa	Linen fibre panel	North	01/10/19	01/10/29	1.5	39	0.0376	0.95	5
MI	Cfa	Linen fibre panel	South	01/10/19	01/10/29	1.5	39	0.0376	0.95	5
MI	Cfa	Linen fibre panel	East/West	01/10/19	01/10/29	1.5	39	0.0376	0.95	5
MI	Cfa	Glass wool	North	01/10/19	01/10/29	1.3	30	0.035	0.99	5
MI	Cfa	Glass wool	South	01/10/19	01/10/29	1.3	30	0.035	0.99	5
MI	Cfa	Glass wool	East/West	01/10/19	01/10/29	1.3	30	0.035	0.99	5
MI	Cfa	Rock wool	North	01/10/19	01/10/29	1.3	119	0.034	0.956	5
MI	Cfa	Rock wool	South	01/10/19	01/10/29	1.3	119	0.034	0.956	5
MI	Cfa	Rock wool	East/West	01/10/19	01/10/29	1.3	119	0.034	0.956	5
MI	Cfa	EPS	North	01/10/19	01/10/29	50	30	0.04	0.95	5
MI	Cfa	EPS	South	01/10/19	01/10/29	50	30	0.04	0.95	5
MI	Cfa	EPS	East/West	01/10/19	01/10/29	50	30	0.04	0.95	5
MI	Cfa	XPS	North	01/10/19	01/10/29	100	40	0.03	0.95	5
MI	Cfa	XPS	South	01/10/19	01/10/29	100	40	0.03	0.95	5
MI	Cfa	XPS	East/West	01/10/19	01/10/29	100	40	0.03	0.95	5

The introduction of the insulating panel in the determined building systems foresees its arrangement in the internal part of the masonry profile, and therefore on the hot side of the masonry under analysis. The choice of the arrangement in this specific configuration arises from the desire to univocally determine the case, insulating the hot side inside, and the existing masonry cold side outside, for each specific type of masonry stratigraphy determined. Besides, simulations will be proposed using a fixed thickness of 5 cm on all the chosen building systems and for any type of insulation adopted. However, different thickness may vary the results reported here.

2.4. Simulation and Orientation Software

The software chosen for data processing was WUFI PRO 6.3.

This software implements a transient heat and mass transfer model. WUFI can be used to determine the distribution of the heat and moisture in a wide range of climatic conditions and building material classes. WUFI allows to determine the drying times of lightweight structures and masonry with trapped or concealed construction moisture, study the influence of driving rain on exterior building components, or investigate the danger of interstitial condensation.

In particular, for this assessment, it is necessary to set the duration period of the simulations. For each of them, a variable calculation of 10 years, starting from 1 October 2019 to 1 October 2029 (87,600 h), has been generated, in order not to interrupt the cold season, which would happen if the simulations were started on 1 January.

The last variable input data necessary for the analysis was the orientation: the simulations were carried out in a variable regime considering the three main orientations (south, north, east/west), thus being able to obtain information related to the cardinal exposure of the wall profiles.

Nevertheless, it should be highlighted that the parts of the ceiling closest to the perimeter wall are places with condensation of water vapour. This is an ideal place for mould to form. This effect should be considered in more depth in further research.

2.5. Definition of Scenarios

The data processing procedure described above was carried out using the WUFI PRO software. In each stratigraphy determined by TABULA (Figure 1), each type of insulation was introduced towards the hot side of the building package with a fixed thickness of 5 cm (Figure 2). For all types of insulation material and building system associated with the location, three simulations were performed, each one associated with a different orientation. The total number of simulations for each chosen city and each insulation applied was 18, for a total of 108 numerical simulations generated, including each building system, city, and orientation (Table 1). Each simulation returned output values related to the maximum percentage of moisture present in the crevice and the MWCI, and these extrapolated data were associated with the period of occurrence in which these phenomena occurred within the wall. Table 2 reports the results for the city of Milan. Table 3 reports masonry layers of the individual building types (with reference to Figure 1).

Table 2. Output data related to the city of Milan associated with the value in percentage of maximum interstitial condensation and water content in the maximum insulation, in the 10 years of simulations.

Scenarios			Output Data			
City	Type of Insulation	Reference Period [dd/mm/yy]	How Long Does It Take to Reach the MAX Value (dd)	MIRH	MWCI	
Milan	Hemp fibre	01/03/21	517	95.91	0.271	
Milan	Hemp fibre	01/03/24	1613	94.85	0.261	
Milan	Hemp fibre	01/03/26	2343	95.44	0.269	
Milan	Linen fibre panel	30/01/25	1948	92.09	0.263	
Milan	Linen fibre panel	01/03/26	2343	90.69	0.255	
Milan	Linen fibre panel	30/01/25	1948	92.09	0.263	
Milan	Glass wool	01/03/21	517	96.57	0.126	
Milan	Glass wool	01/03/25	1978	95.47	0.113	
Milan	Glass wool	01/03/21	517	96.30	0.121	18 simulations for the reference location (Milan)—Output
Milan	Rock wool	01/03/21	517	96.82	0.047	
Milan	Rock wool	02/03/24	1614	96.07	0.046	
Milan	Rock wool	02/03/26	2344	96.56	0.046	
Milan	EPS	03/03/21	519	87.66	0.069	
Milan	EPS	05/02/21	493	84.75	0.062	
Milan	EPS	03/03/21	519	86.62	0.067	
Milan	XPS	03/03/21	519	86.23	0.064	
Milan	XPS	06/02/21	494	83.43	0.058	
Milan	XPS	03/03/21	519	85.18	0.062	
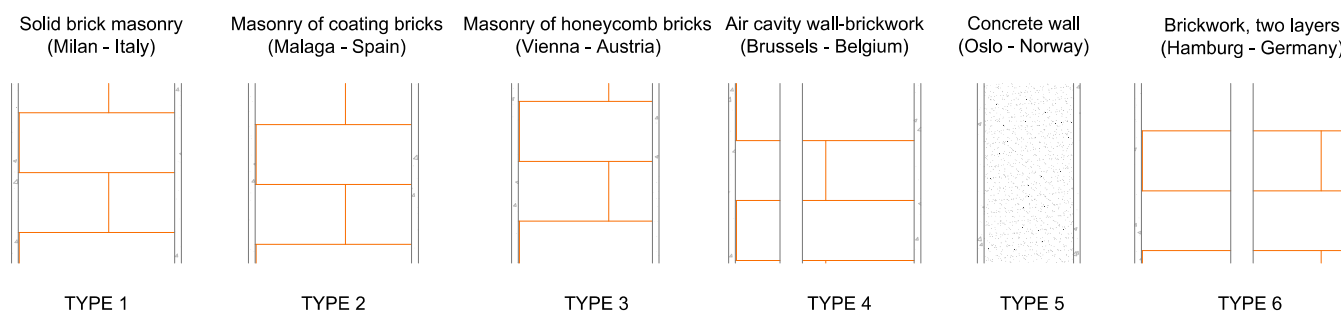
Figure 1. Types of wall stratigraphy determined by TABULA by reference location.

| Solid brick masonry, with internal insulation (Milan - Italy) | Masonry of coating bricks, with internal insulation (Malaga - Spain) | Masonry of honeycomb bricks, with internal insulation (Vienna - Austria) | Air cavity wall-brickwork, with internal insulation (Brussels - Belgium) | Concrete wall, with internal insulation (Oslo - Norway) | Brickwork, two layers, with internal insulation (Hamburg - Germany) |

| TYPE 1 | TYPE 2 | TYPE 3 | TYPE 4 | TYPE 5 | TYPE 6 |

Figure 2. Introduction of the insulating panel in the various types of wall stratigraphy determined by TABULA by reference location.

Table 3. Masonry layers of the individual building types (Figure 1).

|	Type 1	Type 2	Type 3	Type 4	Type 5	Type 6
Masonry layers with insulating panel	Mineral exterior plaster	External cement plaster	Raw exterior plaster	Raw exterior plaster	Raw exterior plaster	External cement plaster
	s = 15 mm	s = 15 mm	s = 15 mm	s = 15 mm	s = 15 mm	s = 15 mm
	Full cooked brick	Cooked brick full load-bearing	Extruded full-cooked brick	Full brick	CLS	Full brick
	s = 350 mm	s = 350 mm	s = 300 mm	s = 100 mm	s = 200 mm	s = 200 mm
	Plaster	Cement plaster	Cement plaster	Layer of air	Plaster	Layer of air
	s = 10 mm	s = 10 mm	s = 10 mm		s = 10 mm	
	Insulation	Insulation	Insulation	Full brick	Insulation	Full brick
	s = 50 mm	s = 50 mm	s = 50 mm	s = 250 mm	s = 50 mm	s = 200 mm
	Internal plaster	Internal plaster	Internal plaster	Plaster	Internal plaster	Plaster
	s = 15 mm	s = 15 mm	s = 15 mm	s = 10 mm	s = 15 mm	s = 10 mm
				Insulation		Insulation
				s = 50 mm		s = 50 mm
				Plaster		Internal plaster
				s = 15 mm		s = 15 mm

3. Results

The results obtained from the numerical simulations in dynamic mode in WUFI PRO have returned the following results, divided as follows:

(a) Climate data.
(b) Data on insulation materials.
(c) Data related to building types.

3.1. Climate Data

The histogram graphs in Figure 3 show: (a) the average and maximum IRH values, expressed as a percentage, by subdivision according to the Köppen system and according to the chosen cities. Graph (a) allows to compare the percentage of humidity between insulation and masonry existing on the *y*-axis, with the climatic subdivision according to the Köppen system on the abscissae axis, representative of the cities considered. Graph (b) shows the WCI values, average and maximum, by subdivision according to the Köppen system and according to the selected cities. The graph allows to compare the amount of water present in the insulation on the *y*-axis with the climatic subdivision according to the Köppen system on the abscissae axis, representative of the cities considered. Table 4 reports the percentages recorded in the different climatic classifications of Köppen, associated with the period of formation of the maximum crevice humidity.
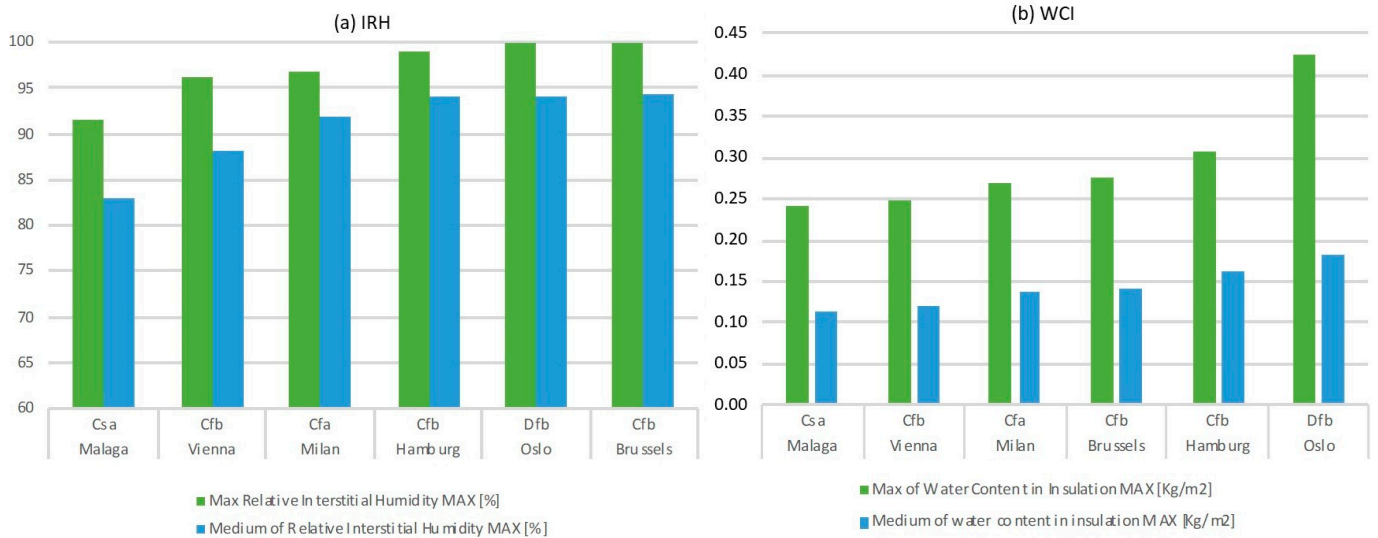
Figure 3. (**a**) Results of IRH values (%), maxima and averages, by subdivision according to the Köppen system. (**b**) Results of WCI values (kg/m^2), maxima and averages, by subdivision according to the Köppen system.

Table 4. MIRH percentages recorded in the different climatic classifications of Köppen, associated with the period of formation of the maximum crevice humidity.

Subdivision According to the Köppen System	Period Associated with the Maximum Interstitial Humidity Value	Maximum Value Reached (%)
Cfb	February 2020	100.00
Csa	February 2021	91.56
Dfb	January 2020/2022/2023/2024/2028/2029 February 2026/2029	100.00
Cfa	March 2021	96.82

3.2. Data on Insulation Materials

The histogram graph in Figure 4 shows along the *y*-axis the values in percentage of the presence of IRH, and in abscissa the types of insulation used divided by location.
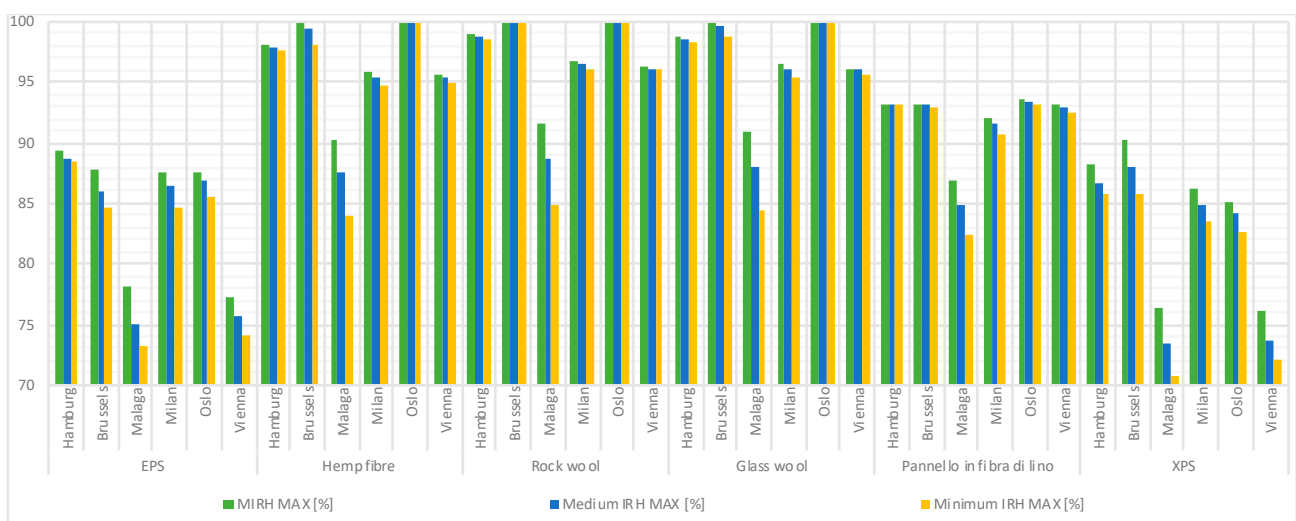
Figure 4. Results of maximum, average, and minimum IRH values (%), broken down by insulation type and application scenario.

The histogram graph in Figure 5 shows the values in kg/m² of the WCI along the *y*-axis, and in abscissa, the types of insulation used divided by location. Table 5 reports the results in terms of orientation, location, and type of insulation of the presence or absence of interstitial condensation between the insulation and existing masonry. Table 6 reports the results in terms of the period of occurrence of interstitial condensation formation by location and type of insulation.
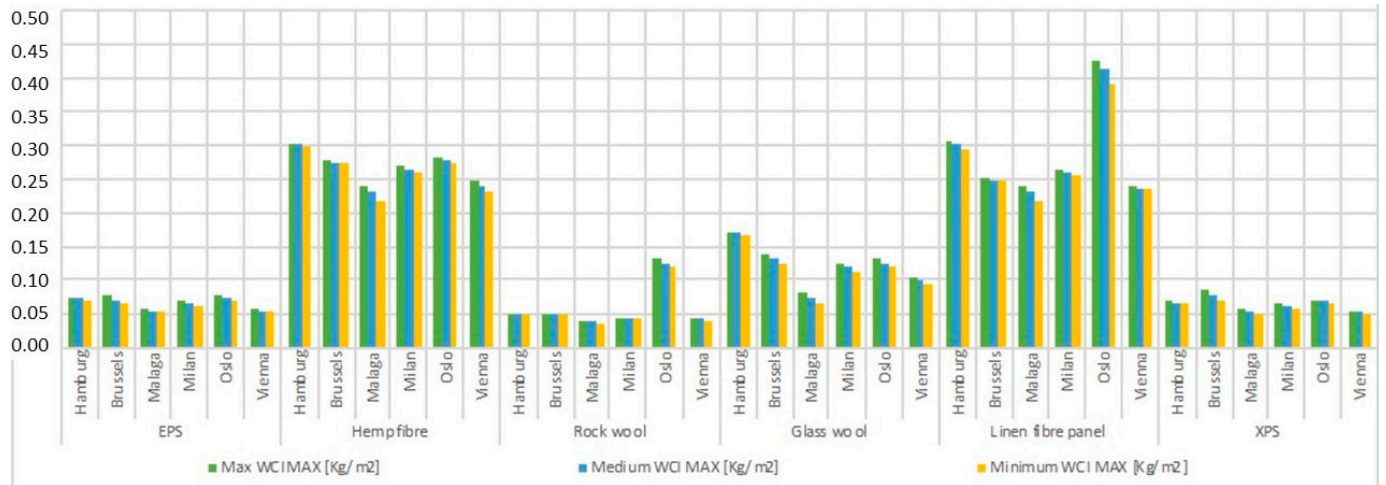

Figure 5. Results of MWCI values, average and minimum (kg/m²), divided by type of insulation and application scenario.

Table 5. Results in terms of orientation, location, and type of insulation of the presence or absence of interstitial condensation between the insulation and existing masonry.

| City	Orientation	Type of Insulation					
		EPS	Hemp Fibre	Rock Wool	Glass Wool	Linen Fibre	XPS
Hamburg	East/West	NO	NO	NO	NO	NO	NO
	North	NO	NO	NO	NO	NO	NO
	South	NO	NO	NO	NO	NO	NO
Brussels	East/West	NO	YES	YES	YES	NO	NO
	North	NO	YES	YES	YES	NO	NO
	South	NO	NO	YES	NO	NO	NO
Malaga	East/West	NO	NO	NO	NO	NO	NO
	North	NO	NO	NO	NO	NO	NO
	South	NO	NO	NO	NO	NO	NO
Milan	East/West	NO	NO	NO	NO	NO	NO
	North	NO	NO	NO	NO	NO	NO
	South	NO	NO	NO	NO	NO	NO
Oslo	East/West	NO	YES	YES	YES	NO	NO
	North	NO	YES	YES	YES	NO	NO
	South	NO	YES	YES	YES	NO	NO
Vienna	East/West	NO	NO	NO	NO	NO	NO
	North	NO	NO	NO	NO	NO	NO
	South	NO	NO	NO	NO	NO	NO

Presence of interstitial condensation ▇. Absence of interstitial condensation ▇.

Table 6. Results in terms of the period of occurrence of interstitial condensation formation by location and type of insulation.

City	Month	Year	Type of Insulation					
			EPS	Hemp Fibre	Rock Wool	Glass Wool	Linen Fibre	XPS
Brussels	February							
		2020	NO	YES	YES	YES	NO	NO
Oslo	January							
		2020	NO	NO	YES	NO	NO	NO
		2022	NO	NO	NO	YES	NO	NO
		2023	NO	NO	YES	NO	NO	NO
		2024	NO	NO	YES	NO	NO	NO
		2028	NO	YES	NO	NO	NO	NO
		2029	NO	YES	NO	YES	NO	NO
	February							
		2026	NO	YES	NO	NO	NO	NO
		2029	NO	NO	NO	YES	NO	NO

Presence of interstitial condensation 🟩. Absence of interstitial condensation 🟥.

The dispersion graphs in Figure 6 represent: (a) the trend of the average density of the insulation (kg/m^3) as a function of the quantity of IRH (%) and (b) the trend of the average density (kg/m^3) concerning the WCI (kg/m^2). The average density has been calculated considering the reference period in which the maximum IRH value occurs in the 10 years of simulation.

(**a**)   (**b**)
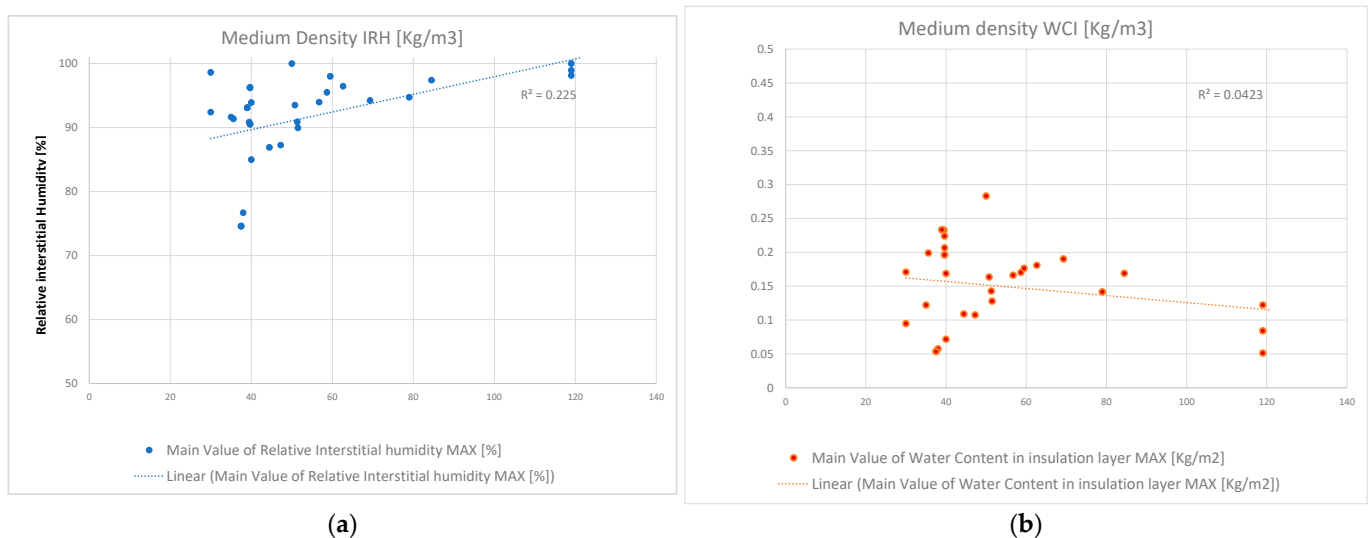
Figure 6. (**a**) Results of the insulation density mean values as a function of the amount of IRH. (**b**) Results of the insulation density mean values as a function of the amount of WCI.

The dispersion graphs in Figure 7 represent: (a) the trend of the vapour permeability coefficient of the insulation (-) as a function of the amount of IRH (%) and (b) the trend of the vapour permeability coefficient of the insulation with respect to WCI (kg/m^2). The average has been calculated with respect to the reference period in which the maximum IRH value occurs in the 10 years of simulation.

The dispersion graphs in Figure 8 represent: (a) the trend of the values relative to the conductivity of the materials in function of the quantity of IRH, where, in abscissae, the values relative to the conductivity (W/mK) are reported, while in ordinate, the values in percentage of the quantity of humidity are shown, and (b) the same trend, however, in ordinate, the quantity of water inside the insulation is reported.
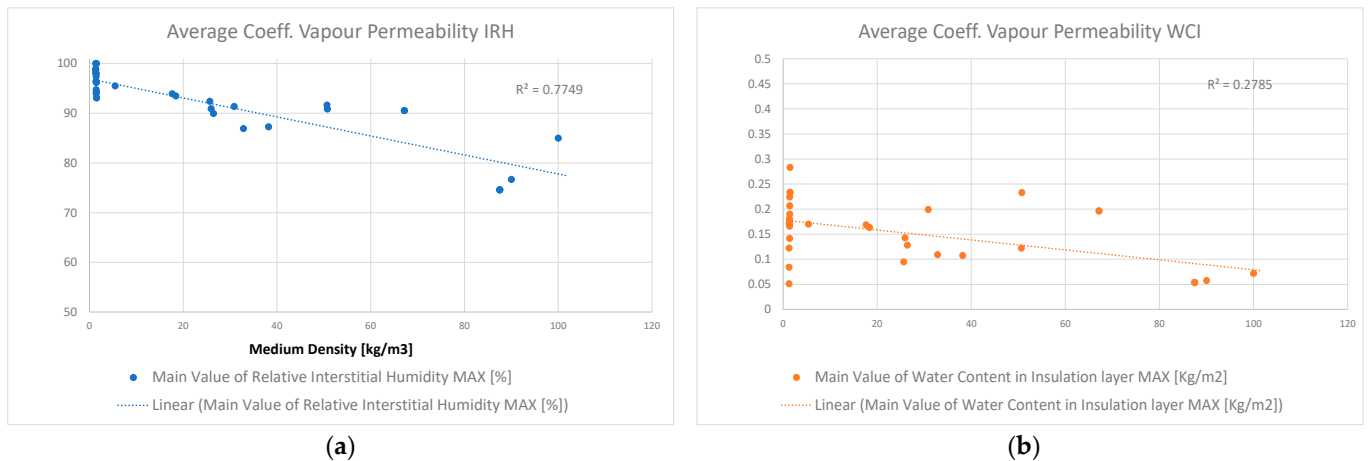
Figure 7. (**a**) Results of the values of the vapour permeability coefficient of the insulation as a function of the amount of IRH. (**b**) Results of the values of the vapour permeability coefficient of the insulation as a function of WCI.
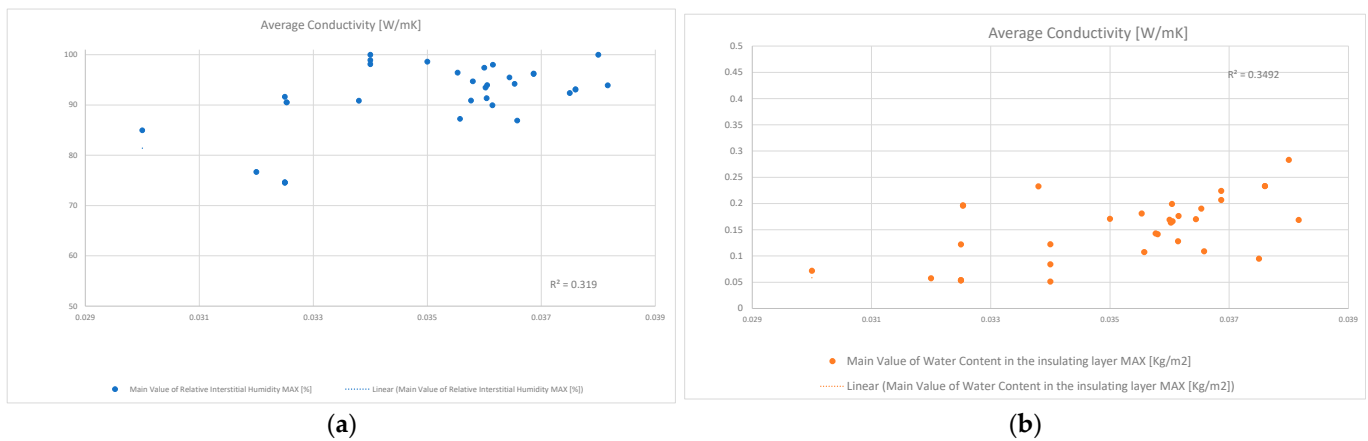
Figure 8. (**a**) Results of the conductivity values of the insulation as a function of the amount of IRH. (**b**) Results of the conductivity values of the insulation as a function of the amount of WCI.

3.3. Data on Building Types

Table 7 shows the representative values of the formation or absence of crevice condensation between the insulation and the existing masonry. The subdivision is expressed by building type and orientation, and these values are interwoven with the types of insulation used in the various building types and the reference locations.

Table 7. Results of the values of the presence of interstitial condensation divided by building type and orientation.

City	Orientation	Type of Insulation					
		EPS	**Hemp Fibre**	**Rock Wool**	**Glass Wool**	**Linen Fibre**	**XPS**
	East/West	NO	NO	NO	NO	NO	NO
Type 1	North	NO	NO	NO	NO	NO	NO
	South	NO	NO	NO	NO	NO	NO
	East/West	NO	NO	NO	NO	NO	NO
Type 2	North	NO	NO	NO	NO	NO	NO
	South	NO	NO	NO	NO	NO	NO

Table 7. *Cont.*

City	Orientation	Type of Insulation					
		EPS	Hemp Fibre	Rock Wool	Glass Wool	Linen Fibre	XPS
Type 3	East/West	NO	NO	NO	NO	NO	NO
	North	NO	NO	NO	NO	NO	NO
	South	NO	NO	NO	NO	NO	NO
Type 4	East/West	NO	YES	YES	YES	NO	NO
	North	NO	YES	YES	YES	NO	NO
	South	NO	NO	YES	NO	NO	NO
Type 5	East/West	NO	YES	YES	YES	NO	NO
	North	NO	YES	YES	YES	NO	NO
	South	NO	YES	YES	YES	NO	NO
Type 6	East/West	NO	NO	NO	NO	NO	NO
	North	NO	NO	NO	NO	NO	NO
	South	NO	NO	NO	NO	NO	NO

Presence of interstitial condensation ▇. Absence of interstitial condensation ▇.

4. Discussion

The results show that the MIRH percentage depends on the climatic context (Köppen) of the city (Figure 3a). The maximum condensation values occurred for the Köppen Cfb (Vienna, Hamburg, Brussels) and Dfb (Oslo) areas; in contrast, for the Cs group (temperate climates with dry summer, Malaga), the IRH value was lower. Likewise, MWCI also depends on the climate zone (Figure 3b), showing that the context and climate zone play a relevant role in the WCI, since as the index of the main group of its classification increased, there was an increase in the value associated with the amount of water. This makes it difficult to standardise applications for different European contexts.

The IRH (Table 4) occurred in the first months of the year, January and February, and in the case of Cfb and Dfb climate zones, 100% saturation between the insulating material and existing masonry was reached. The lower values in terms of IRH were shown to come from the Csa category, where the maximum humidity value was also found in February. For the Dfb areas, it is noted that the presence of interstitial condensation was almost annual in February and January; on the contrary, in the Cfb area, the presence of the latter was uniquely expected for the year 2020, against a numerical simulation lasting 10 years.

The types of insulating material adopted, in the individual climate zones, determined the formation of interstitial condensation between the existing masonry and the thermal insulation (Figure 4). In places such as Oslo and Brussels, the formation of interstitial condensation occurred with the use of hemp fibre insulation, glass wool, and rock wool. For the other configurations, the percentage of humidity never reached saturation. The location with the highest water content in the insulation was Oslo, associated with linen fibre insulation (Figure 5). Since the latter had a lower average density (39 kg/m^3) compared to competing materials, the graph in Figure 6b shows that when the density of the material decreased, there was an increase in terms of total water content in the material. Therefore, the climate has an influential role on the risk of interstitial condensation; indeed, all cities located in adverse climate zones (Cfb, Cfa, Dfb) had high IRH contents, and on the contrary, cities in the driest zones (Csa) had lower values. The formation of condensation, when it occurs, does not depend on the orientation: in all four cardinal configurations were the climatic areas associated with the Dfb zone (Oslo), colder climates; on the contrary, in the other zones (Brussels), the formation of condensation was verified for the north, east, and west orientations, but not always for the south (Table 5). The locations subject to the presence of interstitial condensation were Brussels and Oslo, associated with hemp fibre, glass wool, and rock wool insulation. As far as the city of Brussels is concerned, only stone wool showed the formation of interstitial condensation in all three exposures, while for the other two types of insulation, the southern exposure was free of interstitial condensation.

On the contrary, the city of Oslo had 100% saturation in all three insulators and in all three configurations. Synthetic materials and flax fibre did not cause condensation in any 10-year simulation period, while the materials that promoted condensation were hemp fibre, glass wool, and flax fibre (Table 6).

Materials with high density (kg/m^3) tended to have a higher risk of crevice condensation, while materials with lower density tended to have lower IRH values. In contrast, WCI tended to increase if the density was lower and decrease if the density was higher (Figure 6). As the density increased, there was an increase in the percentage of moisture between the wall and the insulation. The maximum values found were relative to stone wool (with a density of 119 kg/m^3), and this material (as shown in Figure 4) had the highest value in each IRH configuration. On the contrary, the tendency of the values relative to the density of the insulation decreased according to the water content of the insulation (Figure 6b). Indeed, stone wool insulation has a low WCI, although it guarantees the presence of crevice condensation between the existing masonry and the insulation.

The percentage of IRH decreased as a function of the vapour permeability coefficient of the insulation: as the value of the coefficient increased, there was a decrease in the percentage of moisture between the wall and the insulation, and vice versa (Figure 7a). As the value increased, the amount of water inside the insulation became less (Figure 7b). In the limited case in which a material with a high coefficient value was placed (vapour brake), the humidity was stopped before it could reach the existing masonry. Therefore, materials with a high value of the vapour permeability coefficient tend to have a lower risk of relative interstitial condensation, while if this coefficient is tending to zero, the risk of this phenomenon increases. The same consideration is valid for water in the insulation, in fact the latter has the same tendency.

Materials that have an excellent thermal conductivity have less risk of being subject to a high content of IRH; on the contrary, materials that have a low thermal capacity are subject to be more affected by this phenomenon (Figure 8). Table 7 shows that the building types subject to the phenomenon of interstitial condensation were the types 4 and 5 (Table 3). In all the other wall stratigraphies, condensation did not occur. Not all insulating materials led to the presence of condensation; in fact, only for hemp fibre, glass wool, and rock wool was the phenomenon present, while for other insulating materials it did not occur.

5. Conclusions

This research showed that it is possible to relate the results obtained concerning the presence of interstitial condensation and the WCI with the climatic zones according to the Köppen classification, with the nature of the insulating materials, as well as with the building types chosen.

The results showed that there was a close correlation between the risk of interstitial condensation and the climate zones according to the classification; in fact, the categories attributable to this phenomenon concerned only groups C and D, with subgroups Cf and Df, related to temperate climates with a humid summer and cold climates with a humid winter. Specifically, the formation of interstitial condensation has been recorded only for areas Cfb (Brussels) and Dfb (Oslo). The association between materials such as hemp fibre, glass wool, and rock wool with the Cfb and Dfb climate zones favoured the presence of condensation between the existing insulation and masonry only in January and February. The cardinal exposures responsible for the formation of condensation were the north and east/west, in all three insulating materials. The southern exposure was exclusively in the Dfb area (Oslo) for hemp fibre, rock wool, and glass wool, while in the Cfb area (Brussels) for rock wool only. The building types responsible for the formation of interstitial condensation were those associated with the Cfb (Brussels) and Dfb (Oslo) climate zones. Only the stratigraphic characteristics of these types of building systems (Type 4–5), associated with hemp fibre, glass wool, and rock wool insulation, have led to condensation. For the other materials arranged in the same building types, this phenomenon did not occur.

The research also reported output values inherent to the intrinsic properties of individual materials in each climate context, related to IRH and WCI. In fact, it has been shown that IRH tended to increase as the average density of the chosen insulation materials increased, while WCI, on the contrary, tended to decrease as the density value increased. The coefficient of vapour permeability, in relation to the average of the values listed above, has reported that for the percentage of IRH, this value tended to decrease as the latter increased, accordingly with WCI. A similar behaviour, but with the opposite trend, was found when comparing the moisture (%) and water content values with the average conductivity. In fact, as the conductivity value (W/mK) increased, there was an increase of both values.

The obtained results may be useful in identifying the ideal type of insulation material that avoids the formation of interstitial condensation, when it is necessary to ensure an increase in the energy efficiency of the opaque envelope in certain geographical contexts associated with specific building types.

Possible future research could include the possibility of extending this analysis to the case where insulation is available in the external part of the wall stratigraphy, in order to determine which type of configuration could be more advantageous for minimising the risk of interstitial condensation formation.

Author Contributions: Conceptualization, L.T. and K.F.; methodology, L.T. and K.F.; software, K.F.; validation, L.T.; formal analysis, L.T.; investigation, M.C.T.; resources, L.T.; data curation, M.C.T.; writing—original draft preparation, M.C.T.; writing—review and editing, L.T. and M.C.T.; visualization, M.C.T.; supervision, L.T. and K.F.; project administration, L.T.; funding acquisition, L.T. All authors have read and agreed to the published version of the manuscript.

Nomenclature

IRH	Interstitial relative humidity (%)
WCI	Water content in the insulation (kg/m^2)
MIRH	Maximum interstitial relative humidity (%)
MWCI	Maximum water content in the insulation (kg/m^2)
WUFI®	Wärme und Feuchte Instationär
TABULA	Typology Approach for Building Stock Energy Assessment
EUROSTAT	Statistical Office of the European Communities
Cfa	Humid subtropical climate
Csa	Hot-summer Mediterranean climate
Cfb	Temperate oceanic climate
Dfb	Warm-summer humid continental climate
ρ	Material density (kg/m^3)
μ	Vapour resistance coefficient (-)
λ	Thermal conductivity of the material (W/mK)
ε	Material porosity (m^3/m^3)
s	Insulation thickness (cm)

References

1. Ballarini, I.; Corrado, V.; Madonna, F.; Paduos, S.; Ravasio, F. Energy refurbishment of the Italian residential building stock: Energy and cost analysis through the application of the building typology. *Energy Policy* **2017**, *105*, 148–160. [CrossRef]
2. Aste, N.; Angelotti, A.; Buzzetti, M. The influence of the external walls thermal inertia on the energy performance of well insulated buildings. *Energy Build.* **2009**, *41*, 1181–1187. [CrossRef]
3. Lawrence, M. Reducing the environmental impact of construction by using renewable materials. *J. Renew. Mater.* **2015**, *3*, 163–174. [CrossRef]

4.   Kolaitis, D.I.; Malliotakis, E.; Kontogeorgos, D.A.; Mandilaras, I.; Katsourinis, D.I.; Founti, M.A. Comparative assessment of internal and external thermal insulation systems for energy efficient retrofitting of residential buildings. *Energy Build.* **2013**, *64*, 123–131. [CrossRef]

5.   Xu, C.; Li, S.; Zou, K. Study of heat and moisture transfer in internal and external wall insulation configurations. *J. Build. Eng.* **2019**, *24*, 100724. [CrossRef]

6.   Dell'Orto, A. *Isolamento Dall'interno—Sintesi del Quaderno Tecnico n.1 "Soluzioni per Isolare Dall'interno" ad Uso Della Committenza Privata*; Tecnosugheri: Paderno Dugnano, Italy, 2019; pp. 1–13.

7.   Galbusera, G.; Riva, A. *Isolamento Termico Dall'interno senza Barriera al Vapore*; Anit: Milano, Italy, 2013; pp. 1–24.

8.   Latif, E.; Tucker, S.; Ciupala, M.A.; Wijeyesekera, D.C.; Newport, D.J.; Pruteanu, M. Quasi steady state and dynamic hygrothermal performance of fibrous Hemp and Stone Wool insulations: Two innovative laboratory based investigations. *Build Environ.* **2016**, *95*, 391–404. [CrossRef]

9.   Hussain, A.; Calabria-Holley, J.; Lawrence, M.; Jiang, Y. Hygrothermal and mechanical characterisation of novel hemp shiv based thermal insulation composites. *Constr. Build Mater.* **2019**, *212*, 561–568. [CrossRef]

10. Kymäläinen, H.R.; Sjöberg, A.M. Flax and hemp fibres as raw materials for thermal insulations. *Build. Environ.* **2008**, *43*, 1261–1269. [CrossRef]

11. Cristina, B. *Le guide pratiche del Master CasaClima 7-Umidità e tenuta all'aria*; Bozen-Bolzano University Press: Bolzano, Italy, 2014.

12. Csoknyai, T.; Hrabovszky-Horváth, S.; Georgiev, Z.; Jovanovic-Popovic, M.; Stankovic, B.; Villatoro, O.; Szendrő, G. Building stock characteristics and energy performance of residential buildings in Eastern-European countries. *Energy Build.* **2016**, *132*, 39–52. [CrossRef]

13. Corrado, V.; Corgnati, S.P.; Dipartimento, T. *Building Typology Brochure—Italy*; Politecnico di Torino: Turin, Italy, 2014.

14. Ballarini, I.; Corgnati, S.P.; Corrado, V. Use of reference buildings to assess the energy saving potentials of the residential building stock: The experience of TABULA project. *Energy Policy* **2014**, *68*, 273–284. [CrossRef]

15. Ferreira, J.; Duarte Pinheiro, M.; de Brito, J. Refurbishment decision support tools review–Energy and life cycle as key aspects to sustainable refurbishment projects. *Energy Policy* **2013**, *62*, 1453–1460. [CrossRef]

16. TABULA. Available online: http://webtool.building-typology.eu/#bm (accessed on 12 February 2023).

17. Ward, R.D.; Hann, J. Das geographische System der Klimate-Handbuch der Klimatologie 1936. *Bull. Am. Geogr. Soc.* **1911**, *43*, 935. [CrossRef]

18. *EN ISO 13788*; Hygrothermal Performance of Building Components and Building Elements—Internal Surface Temperature to Avoid Critical Surface Humidity and Interstitial Condensation—Calculation Methods. International Organization for Standardization: Vernier, Geneva, 2012.

19. *BS EN 15026*; Hygrothermal Performance of Building Components and Building Elements–Assessment of Moisture Transfer by Numerical Simulation. European Standards: Plzen, Czech Republic, 2007.

20. Cascione, V. *Valutazione Igrotermica di Soluzioni Tecniche D'isolamento Dell'involucro Edilizio per il Recupero Energetico in Italia Per mezzo di Simulazioni Dinamiche*; Politec Di Bari: Bari, Italy, 2016.

21. ASHRAE. *Handbook of Fundamentals*; Criteria for Moisture-Control Design Analysis in Buildings; American Society of Heating, Refrigerating and Air-Conditioning Engineers, Inc.: Atlanta, GA, USA, 2009; Chapter 23; p. 1999.

22. EUROSTAT. Available online: https://ec.europa.eu/eurostat/statistics-explained/index.php/Housing_statistics#Type_of_dwelling (accessed on 12 February 2023).

23. EUROSTAT. Available online: https://ec.europa.eu/energy/en/eu-buildings-database (accessed on 12 February 2023).

24. Kottek, M.; Grieser, J.; Beck, C.; Rudolf, B.; Rubel, F. World map of the Köppen-Geiger climate classification updated. *Meteorol. Zeitschrift.* **2006**, *15*, 259–263. [CrossRef] [PubMed]

25. Bjarløv, S.P.; Finken, G.R.; Odgaard, T. Retrofit with interior insulation on solid masonry walls in cool temperate climates-An evaluation of the influence of interior insulation materials on moisture condition in the building envelope. *Energy Procedia* **2015**, *78*, 1461–1466. [CrossRef]